COMPDYN 2011
III ECCOMAS Thematic Conference on
Computational Methods in Structural Dynamics and Earthquake Engineering
M. Papadrakakis, M. Fragiadakis, V. Plevris (eds.)
Corfu, Greece, 25–28 May 2011

INVESTIGATION OF THE SLIDING RESPONSE OF A RIGID BODY SYSTEM SUBJECTED TO UNI-DIRECTION HORIZONTAL DYNAMIC AND EARTHQUAKE EXCITATIONS

George C. Manos[1], **George Koidis**[1], **and Milton Demosthenous**[2]

[1] Laboratory of Experimental Strength of Materials and Structures, Dept. of Civil Engineering, Aristotle University, Thessaloniki, Greece.
e-mail: gcmanos@civil.auth.gr

[2] Institute of Engineering Seismology and Earthquake Engineering, Thessaloniki, Greece.
demilton@itsak.gr

Keywords: Sliding, Rigid Body, Friction, Seismic Isolation.

Abstract. *An experimental and numerical investigation is presented that studies the sliding response of a rigid body when subjected to horizontal dynamic and earthquake excitations. For this purpose, a steel block mock-up of a rigid body has been constructed and tested at the shaking table of Aristotle University. The dynamic excitations were based on either sinusoidal motions of various amplitudes and frequencies or simulated earthquake excitations based on actual recordings of prototype earthquake ground motions. The experimental results have shown that when sliding of this rigid block is permitted then its peak acceleration response is moderately amplified, provided that the excitation frequency is not close to the resonant frequency range of the block-spring dynamic system. This is particularly true for earthquake excitations and for relatively flexible spring-links thus achieving in this way a type of seismic isolation for the rigid block. A computer software was developed in order to numerically simulated this dynamic sliding response. The numerical results obtained through this specially developed computer software are next compared with the corresponding experimental measurements. The numerically predicted rigid block acceleration response is in good agreement, in all examined cases, with the measured values. The numerically predicted rigid body sliding displacement response also exhibits innumerous cases good agreement with the measured values. However, significant deviation between predicted and measured rigid body sliding displacement amplitudes were also observed. Despite these limitations of the predicted results it is believed that the developed software, although it deals with a complex problem in a relatively simple way, it can be useful in the preliminary design of structural systems with sliding capability at their support.*

1 INTRODUCTION

This paper presents results from an experimental and numerical investigation that deals with the sliding response of a rigid body when subjected to horizontal dynamic and earthquake excitations. The layout of this problem is shown in figure 1, where a rigid body (figure 1, designated with light color) is initially resting on a platform (figure 1, designated with dark color) that can move in a prescribed way in one horizontal direction, thus subjecting the rigid body to horizontal dynamic and earthquake excitations. The contact area between the rigid body and the moving platform is a horizontal plane having a friction coefficient μ (μ_{st}, the static coefficient of friction and μ_d, the dynamic coefficient of friction). Moreover, the rigid body of mass m is connected with the moving platform with an elastic spring having stiffness K and with a damper having a damping coefficient C. The motion of the moving platform is defined by the displacement vector U(t) with respect to an motionless coordinate system x, y whereas the corresponding displacement vector of the rigid body is X(t). The velocity and acceleration vectors of the rigid body and the moving platform are $\dot{X}(t)$ $\ddot{X}(t)$ and $\dot{U}(t)$ $\ddot{U}(t)$, respectively. The sliding displacement between the rigid body and the supporting moving platform is U(t)-X(t). The following are the forces (figure 1) that arise in this rigid body – moving platform dynamic system [1].

F_{ine} = The inertia force, F_{spr} = The spring force , F_{damp} = The damping force
$F_{fr} = \mu_d$ m g = The friction force during sliding
$F_{fr} = \mu_{st}$ m g = The friction force when no sliding occurs

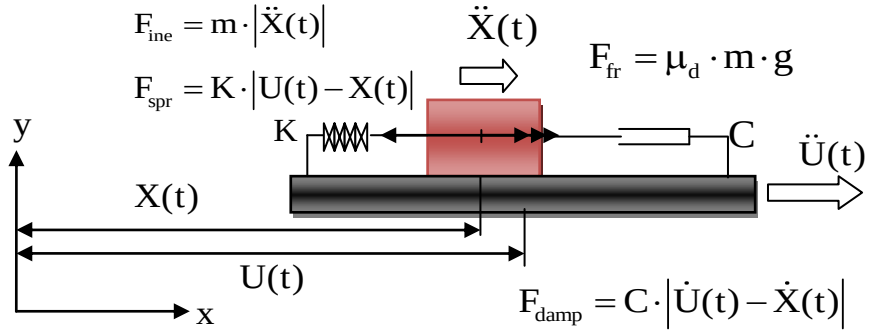

Figure 1. Layout of the problem

This particular problem appears to be of interest either in predicting the dynamic and earthquake response of relatively very stiff objects (rigid) that simple rest on horizontal floors or the behavior of stiff structures that incorporate a sliding surface as means of protection against dynamic or earthquake excitations.

2 EXPERIMENTAL INVESTIGATION

For this purpose, a special mock-up has been constructed that represents physically the previously stated problem (figure 1). It consisted of a steel rigid block rectangular in shape with dimensions 430mm x 430mm in plan and a height either 205mm or 410mm (upper part of figure 2); This block was simply resting on a steel moving platform (lower part of figure 2) and it was restrained to all other directions so that in could move only in the longitudinal horizontal direction. The mass of this sliding rigid block was either 124kg or 248kg. The various important physical parameters for this block sliding response are measured [6], [7], such as the coefficient of friction at the contact surface between the block and the moving

platform and the stiffness of the elastic spring as will be shown in the following sections 2.1. and 2.2. No viscous damper was introduced at this part of the experimental investigation.

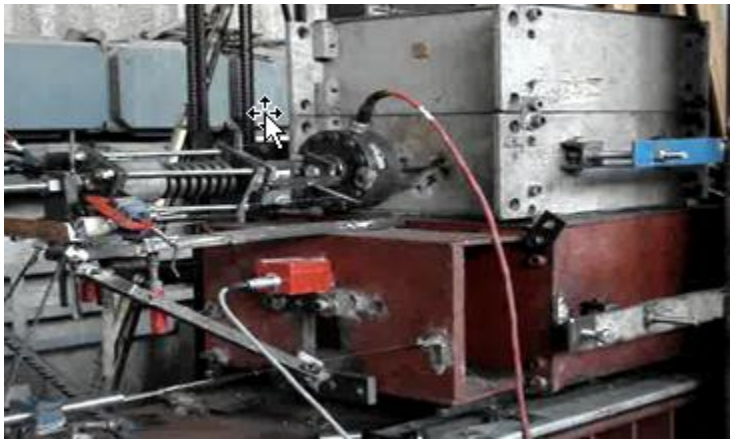

Figure 2. Experimental set-up

2.1 Measuring the coefficient of friction

A special series of tests were performed in order to define the coefficient of friction of the contact surface between the sliding block and the moving platform. This surface was machined in a special way so that full contact conditions could be ensured between the sliding block and the moving platform. Moreover, this contact surface has been lubricated throughout all the experimental sequences [6], [8], [9]. Figure 3 depicts the friction force versus sliding displacement diagram when the mass of the sliding block was equal to 284kg (by placing 36kg extra mass on top of the rigid block). The frequency of the cycling displacements during these tests was varied from 0.1Hz to 1.0Hz. The values for the coefficient of friction found from these tests are listed below. A total number of 10 tests were performed.

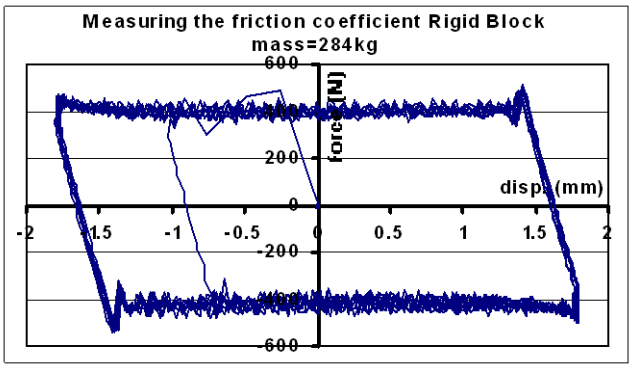

Figure 3. Test for measuring the friction coefficient

When the rigid block mass was equal to 124kg the values of the friction coefficient were:

$\mu_{st} = 0.165$ $\mu_d = 0.153$

When the rigid block mass was equal to 284kg the values of the friction coefficient were:

$\mu_{st} = 0.158$ $\mu_d = 0.136$

2.2 Measuring the stiffness of the spring

Another series of tests were conducted in order to accurately measure the stiffness K of the spring that was employed to link the rigid block to the moving platform, as indicated in figure 1. Two types of springs were tested; the first was a spring that was certified for its properties whereas the second one was not certified. The loading arrangement which is depicted in figure 4 was employed during these tests whereby the force applied on the spring was measured together with the resulting spring displacement. Figure 5a shows the resulting

certified spring response during such a test whereby no pre-stressing force was applied at the spring. In figures 5b and 5c the resulting response is depicted when a pre-stressing force is applied through a special for this purpose system attached to either the certified or the non-certified spring, respectively. As was done for measuring the coefficient of friction, during the tests for measuring the spring stiffness the frequency of the cycling displacement was varied from 0.1Hz to 1.0Hz.

Figure 4. Test for measuring the spring stiffness

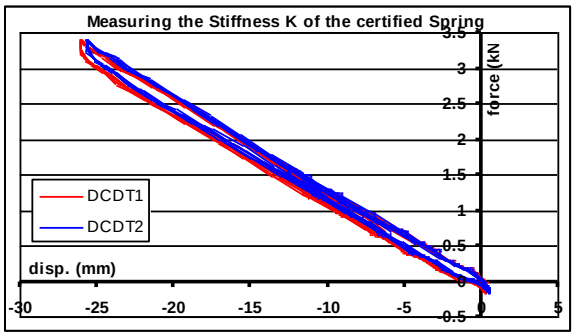

Figure 5a. The certified spring load-displacement response with no pre-stress

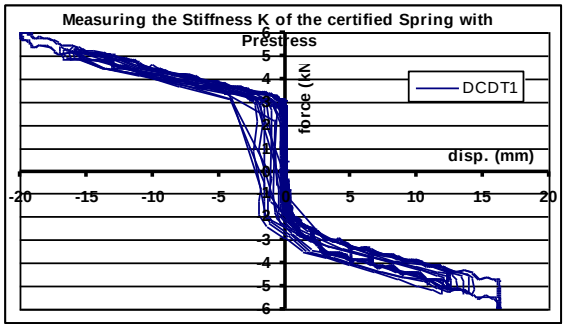

Figure 5b. The certified spring load-displacement response with pre-stress

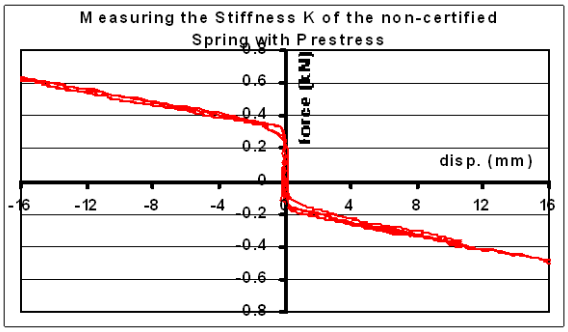

Figure 5c. The non-certified spring load-displacement response with pre-stress

The stiffness of the certified spring with no pres-stress, as was estimated from the load-displacement response of these tests (figure 5a), had an average value K= 128.6 KN/m.

The stiffness of the certified spring with pre-stress, as was estimated from the load-displacement response of these tests (figure 5b), had an average value K= 143 KN/m.

The stiffness of the non-certified spring with pre-stress, as was estimated from the load-displacement response of these tests (figure 5b), had an average value K= 19.4 KN/m.

2.3 Measuring the sliding response of the rigid block

Figure 6 depicts the experimental arrangement, whereby a number of displacement and acceleration sensors were used to monitor the sliding response of the rigid block and the actual motion of the moving platform [6], [7], [8], [9]. The force of the spring link was also monitored. The dynamic excitations of the moving platform were based on sinusoidal motions of various amplitudes and frequencies. The earthquake excitations of the moving platform were laboratory simulations based on actual recordings of prototype earthquake ground motions. The non-certified as well as the certified spring was used in a number of tests with sinusoidal or simulated earthquake excitations. In addition, a number of tests were

also conducted whereby there was no spring link between the rigid block and the moving platform.

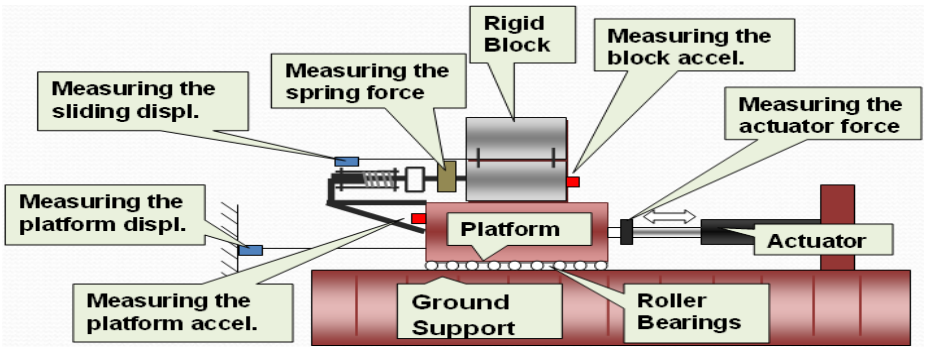

Figure 6. Experimental arrangement for measuring the sliding response of the rigid block.

3 EXPERIMENTAL RESULTS

Selective experimental results are presented in the next sections whereby the rigid block is linked to the moving platform either with the non-certified or with the certified spring or with no spring at all. The moving platform is subjected to either sinusoidal motions, in the frequency range from 0.5Hz to 4Hz, or to simulated earthquake excitations based on the prototype Kern Country 1953 prototype earthquake horizontal acceleration recording (HTaft0407.int). The non-certified spring with a pre-stressing force is used in section 3.1. The results that are presented in this section are for a test that used a sinusoidal motion of 1.5Hz for the moving platform. The certified spring with no pre-stressing force is used in section 3.2. The results that are presented in this section are for a test that used a sinusoidal motion of 3.0Hz for the moving platform whereas in section 3.3. the certified spring with no pre-stress is again employed but this time the above named simulated earthquake motion is utilized. Finally, in sections 3.4. and 3.5. there is no spring linking the rigid block with the moving platform; a sinusoidal motion of 1.5Hz is employed in section 3.4. whereas the above named simulated earthquake motion is utilized in section 3.5.

3.1 Sinusoidal excitation 1.5Hz with non-certified spring (with pre-stress)

The presented results include the acceleration response (m/sec^2) of the moving platform and of the sliding rigid block (figure 7a) whereas the displacement (mm) of the moving platform and the spring is depicted in figures 7b and 7d respectively. Figures 7c and 7e depict the force that develops at the spring (KN) as well as the force-displacement response of this spring. Finally figure 7f depicts the sliding displacement of the rigid block relatively to the moving platform. Obviously, this sliding displacement must be theoretically equal to the spring displacement; this practically materializes in the used experimental set-up as can be seen by comparing the displacement response of figures 7f and 7d. Moreover, it can be seen that the non-certified spring force-displacement response with pre-stress measured individually (figure 5c) is in good agreement with that measured during the sliding response of the rigid body that mobilizes the response of the spring (figure 7e)

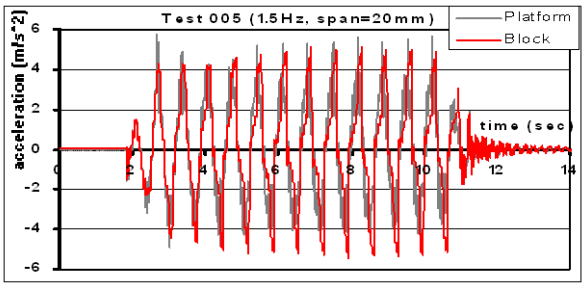

Fig. 7a. Acceleration response of moving platform (ground) and of the sliding rigid block .

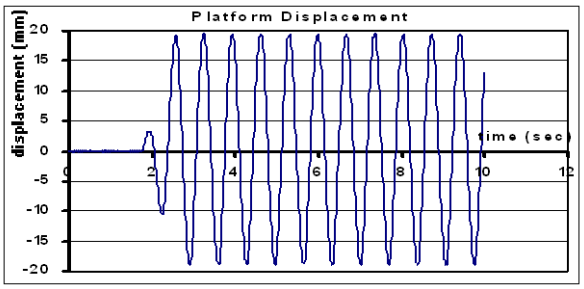

Fig. 7b. Displacement of the moving platform, (Test 005 29-11-2007)

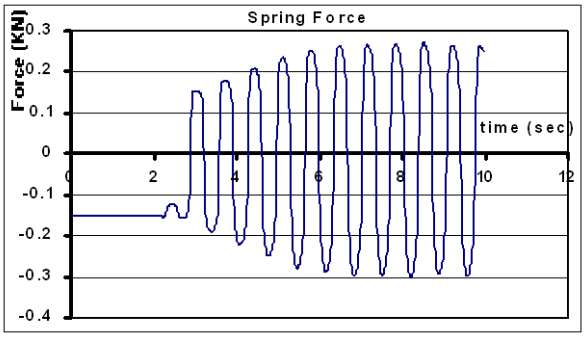

Fig. 7c. Force that was measured at the spring

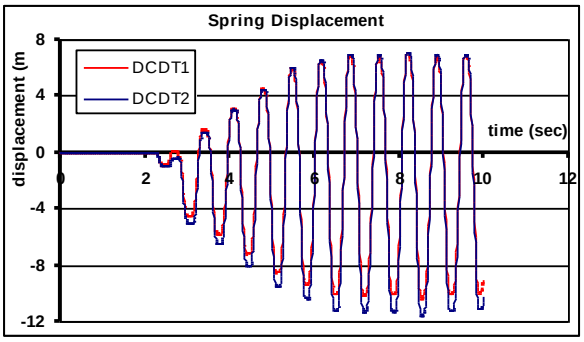

Fig. 7d. Displacement of the spring

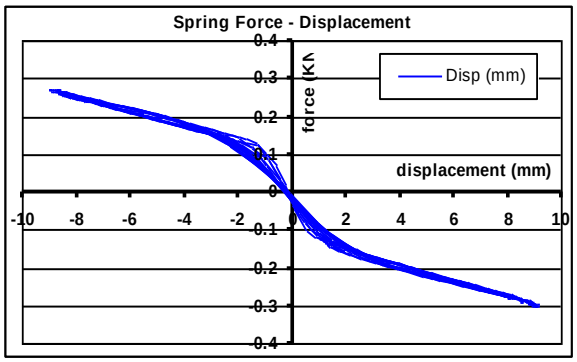

Fig. 7e. Force-displacement response of the spring

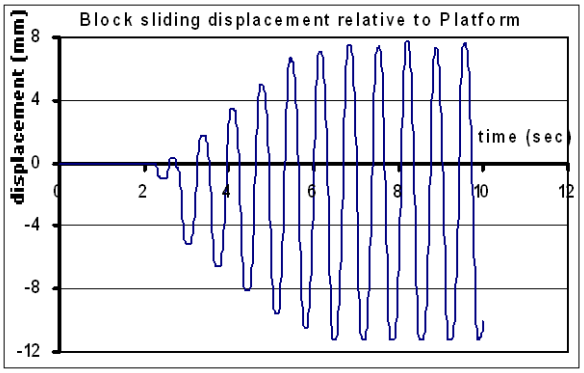

Fig. 7f. Sliding displacement of the rigid block relative to the moving platform

3.2 Sinusoidal excitation 3.5Hz with certified spring (no pre-stress)

Again, the presented results include the acceleration response (m/sec²) of the moving platform and of the sliding rigid block in figure 8a whereas the displacement (mm) of the moving platform and the spring is depicted in figures 8b and 8d respectively. Figures 8c and 8e depict the force that develops at the spring (KN) as well as the force-displacement response of this spring. Moreover, it can be seen that the certified spring response with no pre-stress measured during the sliding response of the rigid body that mobilizes the response of the spring (figure 8e) is in good agreement with that measured individually (figure 5a).

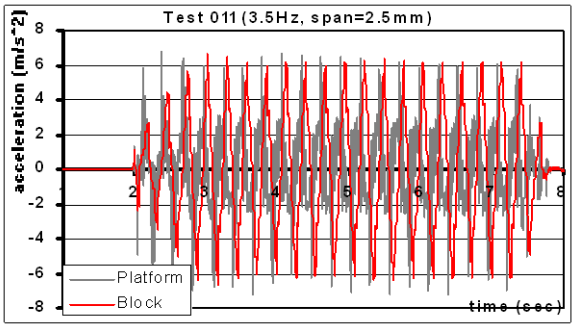

Fig. 8a. Acceleration response of the moving platform and of the sliding block

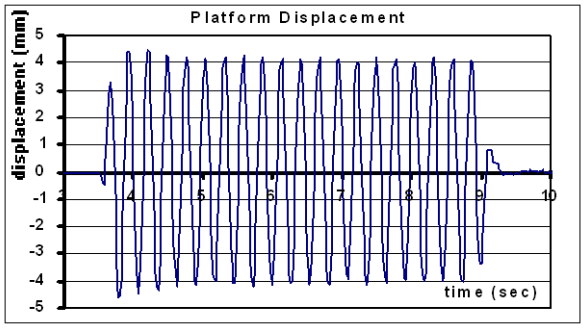

Fig. 8b. Displacement of the moving platform, Test 011, 19-12-2007

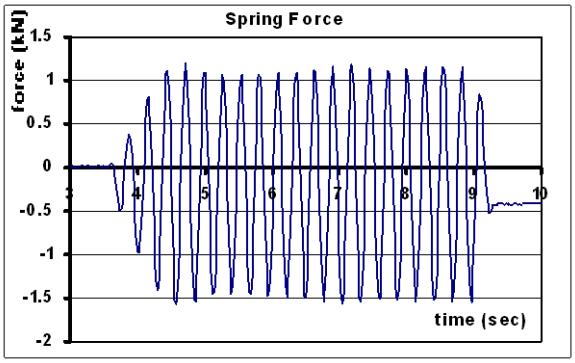

Fig. 8c. Force that was measured at the spring

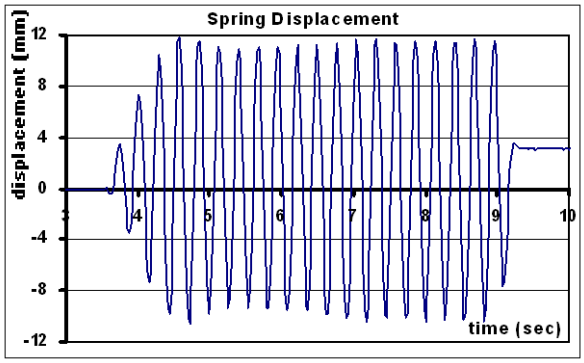

Fig. 8d. Displacement of the spring and sliding displacement of the rigid block

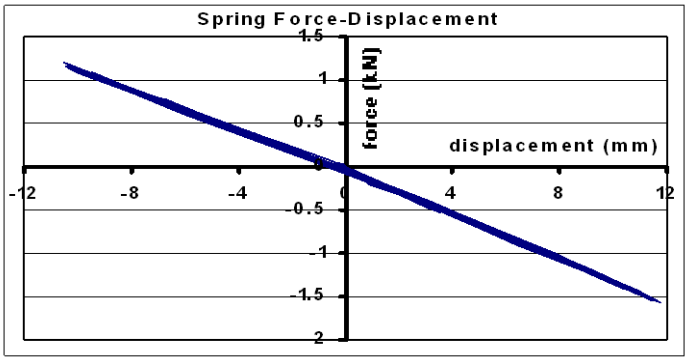

Fig. 8e. Force-displacement response of the spring

3.3 Simulated earthquake excitation with certified spring.

The results of two tests are presented here, both conducted with the certified spring; they are Test 002 (with small pre-stress, figures 9a to 9e) and Test 004 (with no pre-stress, figures 10a to 10e). Again, the presented results include the acceleration response of the moving platform and of the sliding rigid block in figures 9a (small pre-stress) or in figure 10a (no pre-stress). The displacement of the moving platform is depicted in figures and the spring is depicted in figures 9b (small pre-stress) or in figure 10b (no pre-stress). Figures 9d and 10d depict the displacement of the spring, which coincides with the sliding displacement of the rigid block, whereas figures 9c and 10c depict the corresponding spring force. The force-displacement response of this certified spring is depicted in figures 9e and 10e, for either the small pre-stress or the no-pre-stress case, respectively. These force displacement response curves can be compared again with figures 5b and 5a, whereby a relatively good agreement can again be observed. Moreover, it can be seen that due to sliding the maximum acceleration response that develops at the rigid block is much smaller than the maximum

acceleration response of the moving platform (figures 9a and 10a). However, this reduction in the acceleration response of the rigid block is accompanied with considerable sliding displacement response of the rigid block that attains a maximum value equal to 3.65mm for Test 002 and to 14mm for Test 004.

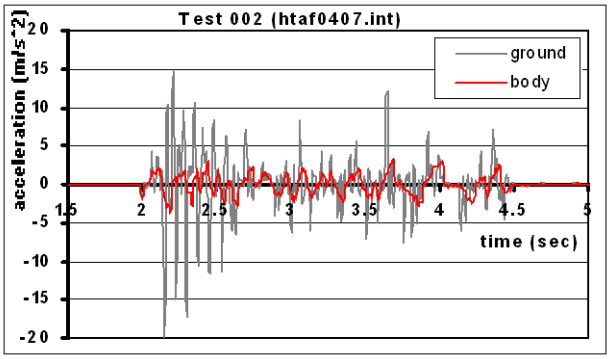

Fig. 9a. Acceleration response of the moving platform and of the sliding block

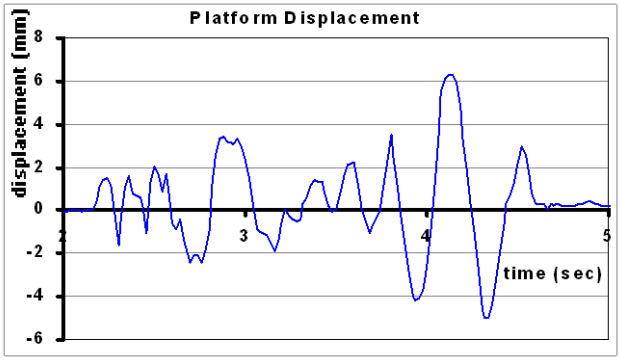

Fig. 9b. Displacement of the moving platform, Test 002, 21-12-2007

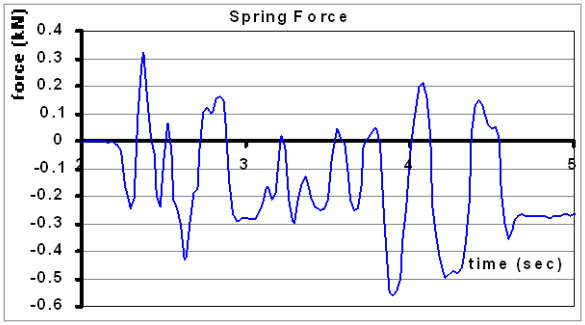

Fig. 9c. Force that was measured at the spring

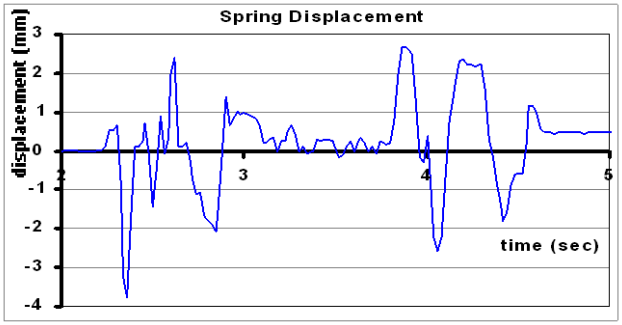

Fig. 9d. Displacement of the spring – rigid block sliding displacement

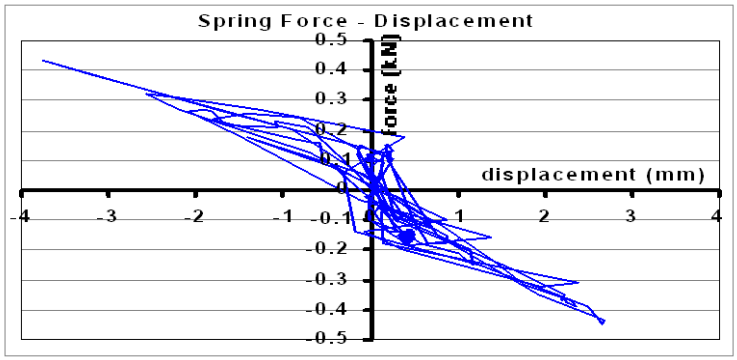

Fig. 9e. Force-displacement response of the spring

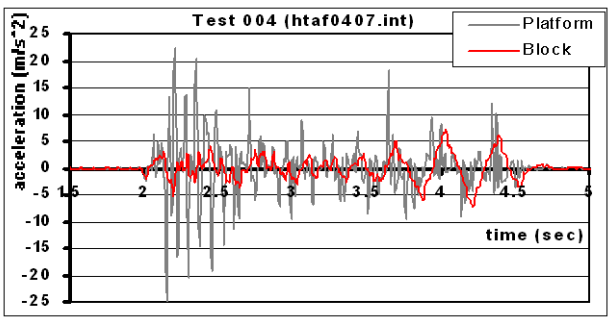

Fig. 10a. Acceleration response of the moving platform and of the sliding block

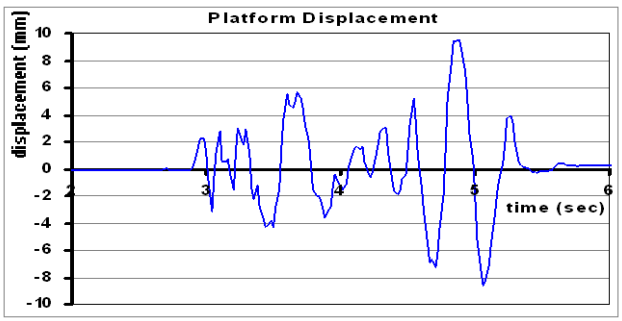

Fig. 10b. Displacement of the moving platform, Test 004, 21-12-2007

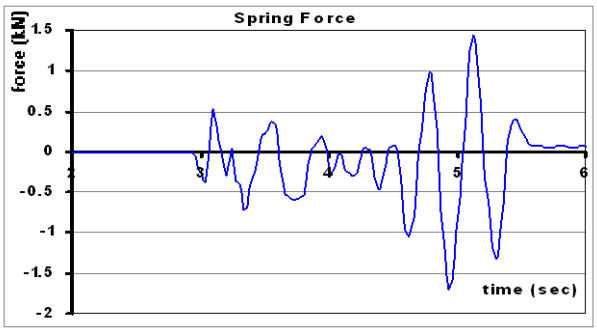

Fig. 10c. Force that was measured at the spring

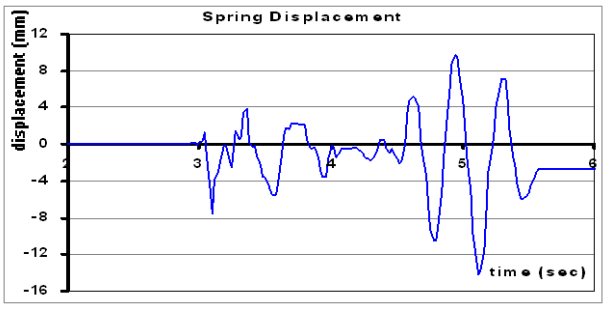

Fig. 10d. Displacement of the spring – rigid block sliding displacement

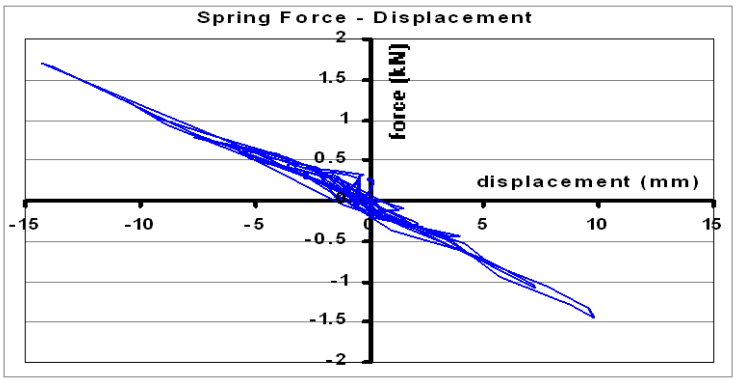

Fig. 10e. Force-displacement response of the spring

3.4 Sinusoidal excitation 1.5Hz without spring link.

In this section as well as in the next section 3.5 the rigid block is simply resting on the moving platform having removed the spring that linked during the previous experiments the rigid block with the moving platform. In the present section the platform is moving in a horizontal sinusoidal motion of 1.5Hz.

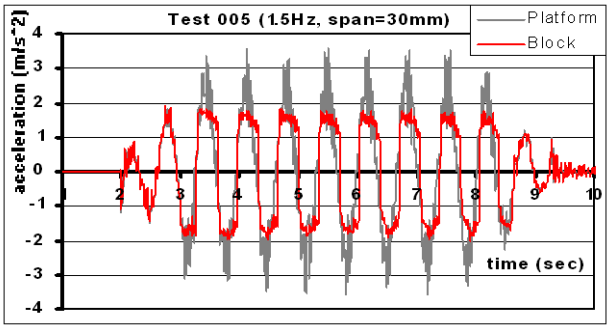

Fig. 11a. Acceleration response of the moving platform and of the sliding block

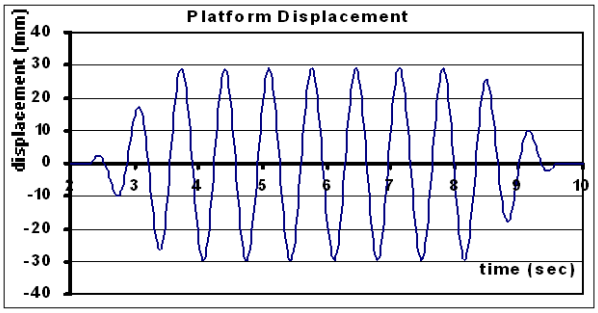

Fig. 11b. Displacement of the moving platform, Test 005, 14-1-2008

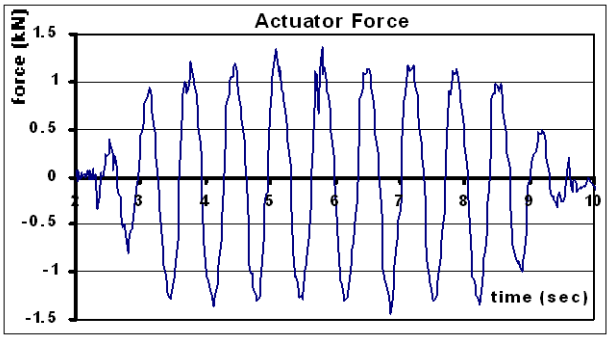

Fig. 11c. Force that was measured at the actuator

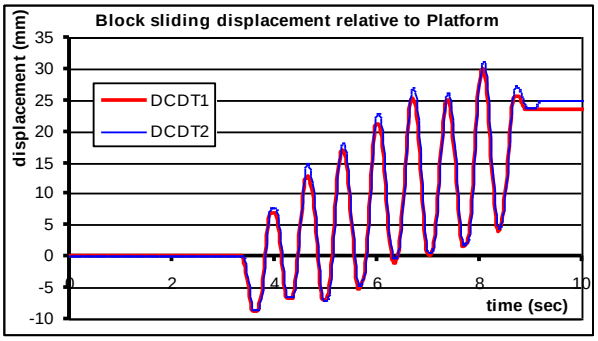

Fig. 11d. Sliding displacement of the rigid block

The acceleration response of the moving platform and of the sliding rigid block is depicted in figure 11a whereas the displacement of the moving platform and the sliding displacement of the rigid block is depicted in figures 11b and 11d respectively. Figure 11c depicts the force that develops at the actuator during this experiment. In this case of free sliding, the maximum rigid block acceleration response is theoretically equal to $\mu_d \cdot g$, which is approximately confirmed by the measured response (if it processed with the proper low-pass filter). It is interesting to note that, in the absence of the spring link, the sliding displacement response of the rigid block develops relatively large values (30mm); moreover, there is a cumulative sliding displacement that appears as an offset from the initial zero displacement condition. This may be attributed to manufacturing tolerances whereby the contact surface between the rigid block and the moving platform deviates from the ideal horizontal plane. This deviation, which was beyond the means of our laboratory checking capabilities, may be also present in actual in-situ applications. The presence of the spring during the previous sinusoidal tests (section 3.1. and 3.2.) has as a result the reduction of the maximum sliding displacement values and the symmetric sliding with respect to the initial zero displacement condition (no cumulative sliding, see figures 7f and 8d). As was observed in all the previously depicted experiments the acceleration response of the rigid block is smaller than that of the moving platform.

3.5 Simulated earthquake excitation without spring link.

Again, the rigid block is simply resting on the moving platform having removed the spring-link. This time, the moving platform is subjected to a simulated earthquake excitation based on the prototype Kern Country 1953 prototype earthquake horizontal acceleration recording (HTaft0407.int).

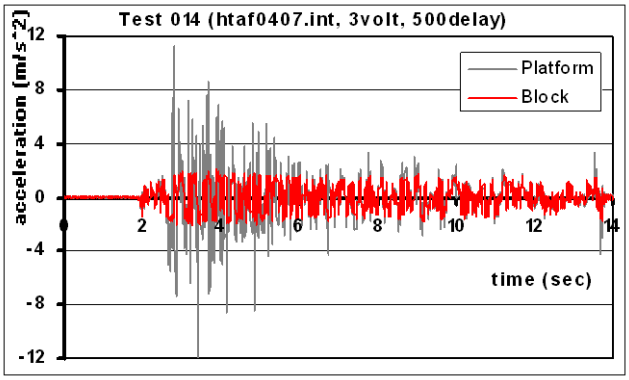

Fig. 12a. Acceleration response of the moving platform and of the sliding block

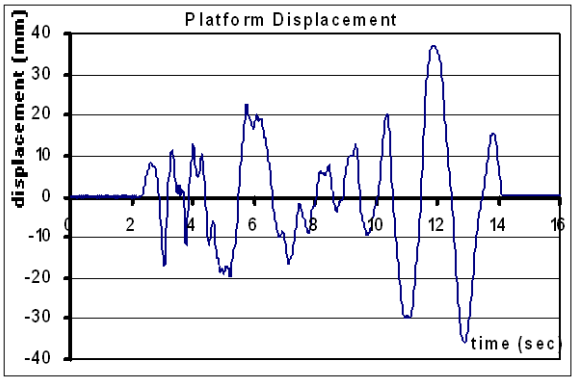

Fig. 12b. Displacement of the moving platform, Test 014, 14-1-2008

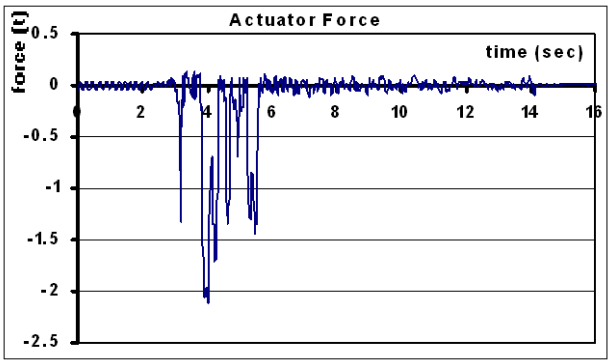

Fig. 12c. Force that was measured at the actuator

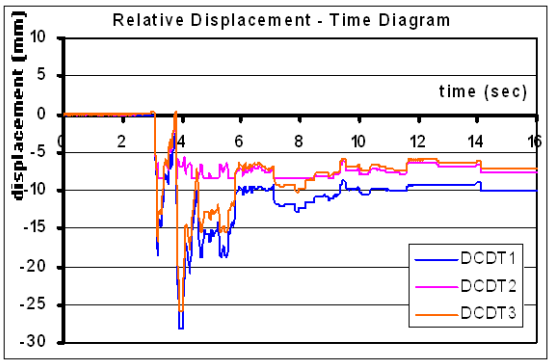

Fig. 12d. Sliding displacement of the rigid block relative to the moving platform

As before, the presented results include the acceleration response of the moving platform and of the sliding rigid block in figure 12a whereas the displacement of the moving platform and the spring is depicted in figures 12b and 12d, respectively. It can be seen that, due to sliding of the block without the spring link, the maximum rigid block acceleration response is much smaller than the maximum moving platform acceleration response (figure 12a). It is again interesting to note that in the absence of the spring link, the sliding displacement response of the rigid block develops relatively large values (30mm), as was also observed in section 3.4; moreover, there is again a cumulative sliding displacement that appears as an offset from the initial zero displacement condition. As mentioned in the previous section, this may be attributed to manufacturing tolerances whereby the contact surface between the rigid block and the moving platform deviates from the ideal horizontal plane. The sliding displacement response of the rigid block without the spring develops maximum sliding almost 30mm (figure 12d) which is twice as much as the sliding response of the rigid block linked to the moving platform with the certified spring and subjected to the simulated earthquake motion of HTaft0407.int (15mm, figure 10d, section 3.3).

4 NUMERICAL INVESTIGATION

The basic conditions, which are given below, are governing the sliding of the rigid body that is linked with a spring (K) and a damper (C) to a moving platform when it is subjected to horizontal $\ddot{U}(t)$ and vertical $\ddot{V}(t)$ acceleration. This represents the most general two dimensional rigid body sliding set-up [1], [2], [3], [4], [5].
Starting from an initial condition of no motion, in order for the rigid body to start sliding the platform acceleration $\ddot{U}(t)$ must exceed the value given by the following inequality (1)

$$\left|\ddot{U}(t)\right| > \mu_{st} \cdot g \cdot \left(1 + \frac{\ddot{V}(t)}{g}\right) \quad (1)$$

In this case, the rigid body acceleration will be given by the following relationship (2):

$$\ddot{X}(t) = \mu_d \cdot g \cdot \left(1 + \frac{\ddot{V}(t)}{g}\right) \cdot \left[\text{sign}\left(\dot{U}(t) - \dot{X}(t)\right)\right] + \frac{K}{m} \cdot \left(U(t) - X(t)\right) + \frac{C}{m} \cdot \left(\dot{U}(t) - \dot{X}(t)\right) \quad (2)$$

When the rigid body is sliding it will be checked for reattachment to the moving platform by examining the absolute value of its relative velocity $\left|\dot{U}(t) - \dot{X}(t)\right|$, e.g. the relative velocity of the rigid body to the moving platform. If the value of the relative velocity becomes equal to zero and inequality (3) holds the rigid body will keep sliding.

$$\text{If } \left|\dot{U}(t) - \dot{X}(t)\right| = 0 \text{ and } \left|\ddot{U}(t) - \frac{K}{m} \cdot \left(U(t) - X(t)\right)\right| > \mu_{st} \cdot g \cdot \left(1 + \frac{\ddot{V}(t)}{g}\right) \quad (3)$$

If the value of the relative velocity becomes equal to zero and inequality (4) holds the rigid body is reattached to the moving platform

$$\text{If } \left|\dot{U}(t) - \dot{X}(t)\right| = 0 \text{ and } \left|\ddot{U}(t) - \frac{K}{m} \cdot \left(U(t) - X(t)\right)\right| \le \mu_{st} \cdot g \cdot \left(1 + \frac{\ddot{V}(t)}{g}\right) \quad (4)$$

The above conditions were included in a computer software (namely *block* and *blockr*) that used a time step-by-step integration procedure incorporating an iteration scheme to reach acceptable limits of convergence. In this step-by-step integration procedure the following

simple relationships (5) and (6) were used for defining the velocity and displacement at a time t_i for the rigid body.

$$\dot{X}(t_i) = \dot{X}(t_{i-1}) + \left(\ddot{X}(t_{i-1}) + \ddot{X}(t_i)\right)\cdot\frac{\Delta t}{2} \quad (5)$$

$$X(t_i) = X(t_{i-1}) + \left(\dot{X}(t_{i-1}) + \dot{X}(t_i)\right)\cdot\frac{\Delta t}{2} \quad (6)$$

This computer software was next validated by numerically simulating the dynamic sliding response of the tested rigid block and by comparing the measured in the laboratory response, as briefly presented and discussed in sections 3.1. to 3.5 with the corresponding numerical predictions. In this numerical simulation all the important physical parameters of the problem at hand, such as the friction coefficients, the spring stiffness, the rigid body mass and the moving platform motion, were given as input to this computer software with values that were found from the laboratory measurements. The numerical results that describe the sliding response of the rigid block, obtained through this software, are next compared with the corresponding test results in the following sections 4.1. to 4.5.

4.1 Comparison of numerical predictions with the response measured during the test employing sinusoidal excitation 1.5Hz with non-certified spring (with pre-stress)

Figure 13a,b depicts a comparison of the predicted by the block software acceleration response of the rigid block with the corresponding measured response during this test when the moving platform is subjected to a sinusoidal motion of 1.5Hz. Apart from the platform motion that is input to the software the rest of the input parameters, are listed in figures 13a,b such as the static (μ_{st}) and dynamic coefficient (μ_d) of friction, the mass of the rigid block (M) and the stiffness of the spring.

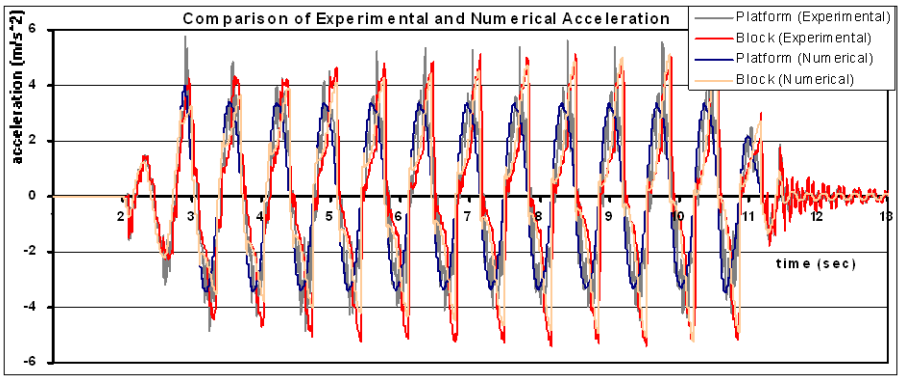

block (no-prestress)

Input parameters
μst= .32 , μd= .27
K (N/m)= 20500
M (kg)= 248
DtF (sec)= .005
Dt (sec)= .001
TIME (sec)= 14.995

Fig. 13a.

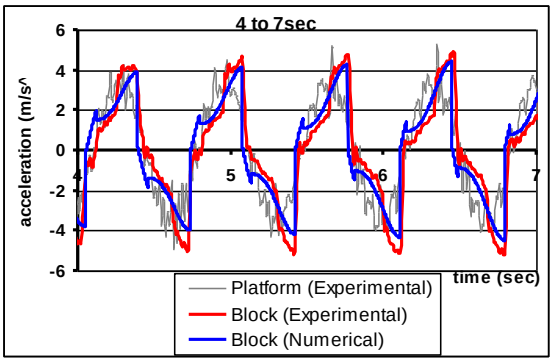

Fig. 13b block (no-prestress) K (N/m)= 20500

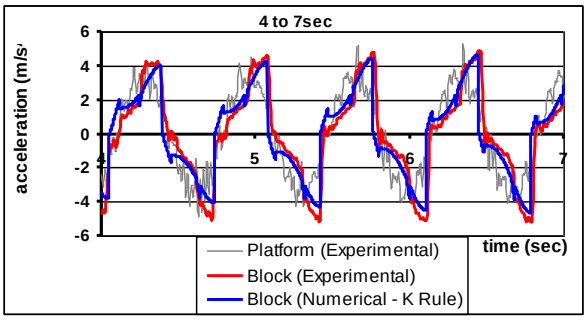

Fig. 13c blockr (pre-stress) K1 (N/m) = 58000
K2 (N/m) = 21500

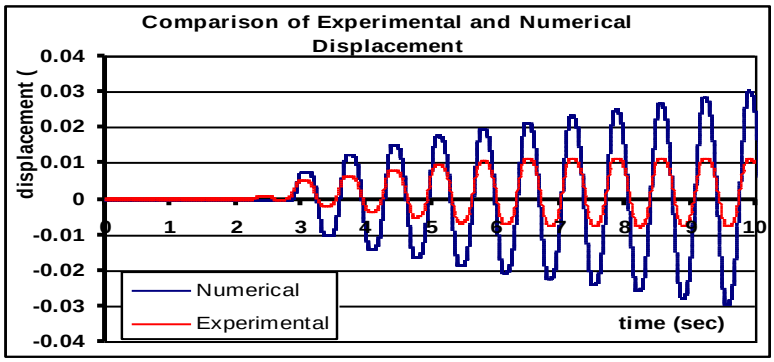

Figure 13d. Block sliding displacement response (Test 005 29-11-2007)

The stiffness of the spring is denoted as K when no pre-stress is present and K1/K2 when the spring is pre-stress and this is taken into account in the software (blockr). Figure 13a represents this measured and predicted rigid block acceleration response for the whole duration of the performed experiment whereas figure 13b and 13c represent time windows of this response between 4 and 7seconds of the total time history. For predicting the rigid block acceleration response the spring pre-stress was initially ignored (figure 13b) and then it was taken into account (figure 13c). In the same figure the measured acceleration of the moving platform is also plotted together with the input platform acceleration used by the software.

As can be seen in figure 13b a relatively good agreement is obtained between predicted and measured rigid block acceleration response which is further improved when the spring pre-stress is included in the software (figure 13c). In figure 13d, the predicted sliding displacement response of the rigid block is compared with the corresponding measured response for the same test. As can be seen, the predicted sliding displacement response is significantly larger than the one measured in the laboratory.

4.2 Comparison of numerical predictions with the response measured during the test employing sinusoidal excitation 3.5Hz with certified spring (no pre-stress)

The comparison between predicted and measured rigid block acceleration response is presented in figures 14a,b as was done in the previous section whereas the predicted rigid block sliding response is presented in figure 14c.

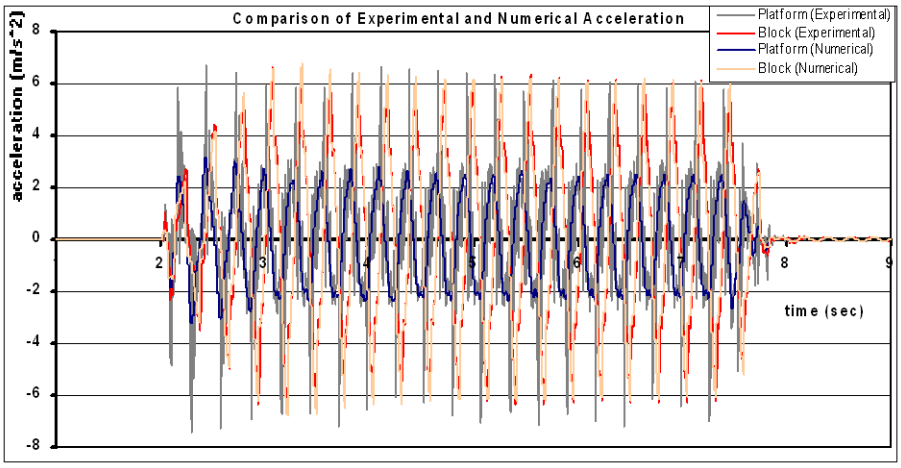

block (no-prestress)

Input parameters

μst= .15
μd= .145
K (N/m)= 100000
M (kg)= 248
DtF (sec)= .005
Dt (sec)= .0005
TIME (sec)= 10.005

Fig.14a. Acceleration response of moving platform and of the sliding rigid block (Test 011, 19-12-2007)

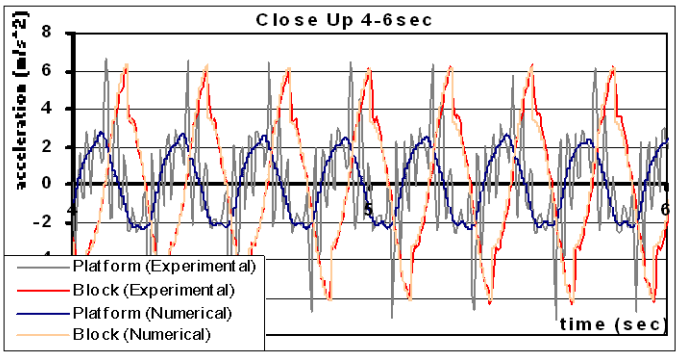

Fig. 14b Acceleration response of moving platform and of the sliding rigid block (Test 011, 19-12-2007)

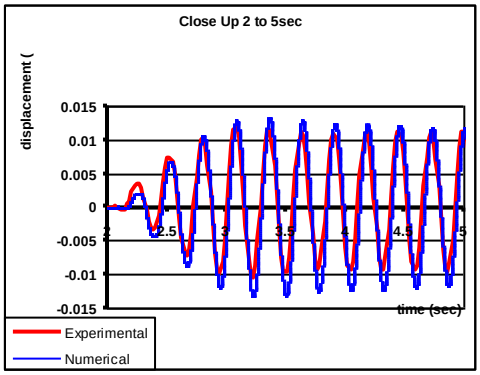

Figure 14c. Rigid block sliding displacement response (Test 011, 19-12-2007)

As can be seen in figures 14a,b good agreement is obtained between predicted and measured rigid block acceleration response. In figure 14c, the predicted sliding displacement response of the rigid block is compared with the corresponding measured response for the same test. As can be seen, this time very good agreement is obtained between the predicted rigid block sliding displacement response and the one measured in the laboratory.

4.3 Comparison of numerical predictions with the response measured during the test employing simulated earthquake excitation with non-certified spring (with pre-stress)

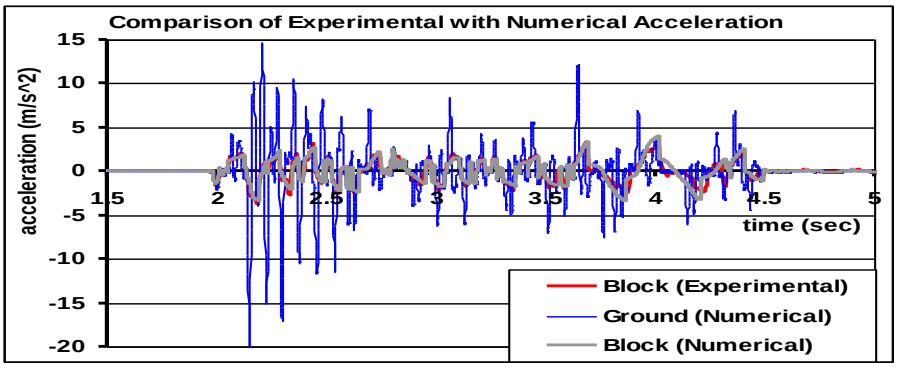

Input parameters
μst= .15
μd= .13
K (N/m)= 123000
M (kg)= 248
DtF (sec)= .005
Dt (sec)= .001
TIME (sec)= 5.495

Fig. 15a. Acceleration response of moving platform and of the sliding rigid block (Test 002, 21-12-2007

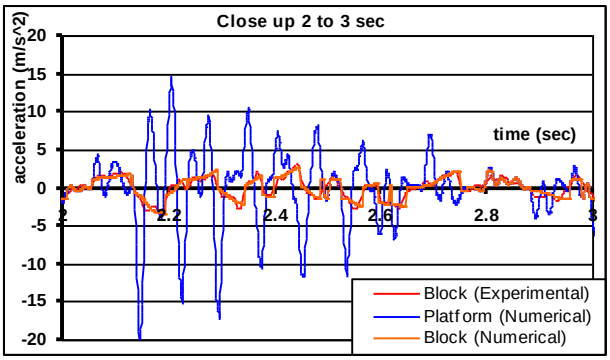

Fig. 15b. Acceleration response of moving platform and of the sliding rigid block (Test 002, 21-12-2007)

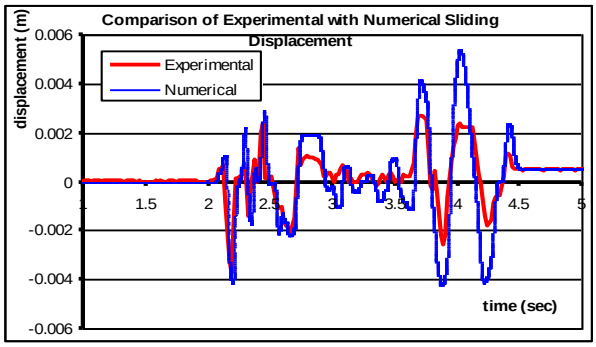

Fig. 15c. Sliding displacement response of rigid block (Test 002, 21-12-2007)

The comparison between predicted and measured rigid block acceleration response is presented in figures 15a,b as was done in the previous sections, whereas the predicted rigid block sliding displacement response is presented in figure 15c. The rigid block is linked to

the moving platform with the non-certified spring (with pre-stress). This time the excitation is a simulated earthquake motion (see section 3.3). As can be seen, good agreement is obtained between predicted and measured rigid block acceleration response. The predicted rigid block sliding displacement response correlates reasonably well with the one measured in the laboratory in the time domain. However, the predicted sliding displacement response, in terms of amplitude, is significantly larger than the one measured in the laboratory.

The measured response is again compared with the one predicted by the software in figures 16a,b,c for a simulated earthquake test (Test 004, 21-12-2007), which is more intense than the one used before (Test 002, 21-12-2007). This time, the good agreement between observed and predicted rigid block response can be seen for both the acceleration (figures16a,b) as well as the sliding displacement response (figure 16c)

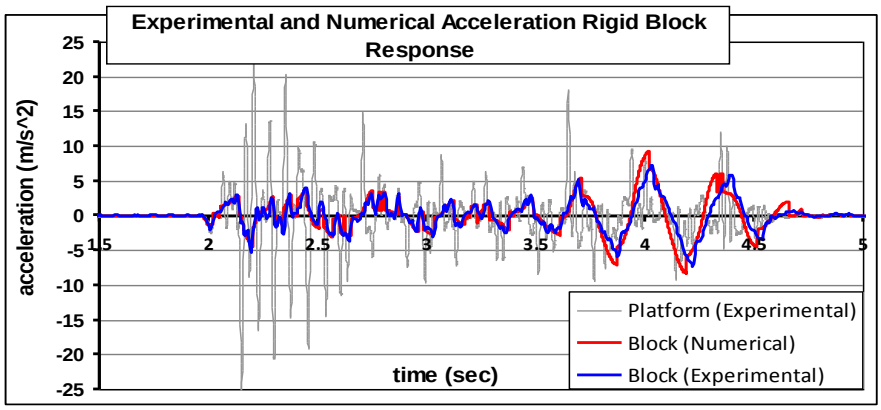

Input parameters
μst= .15
μd= .13
K (N/m)= 120000
M (kg)= 248
DtF (sec)= .005
Dt (sec)= .001
TIME (sec)= 5.995

Fig. 16a. Acceleration response of moving platform and of the sliding rigid block (Test 004, 21-12-2007

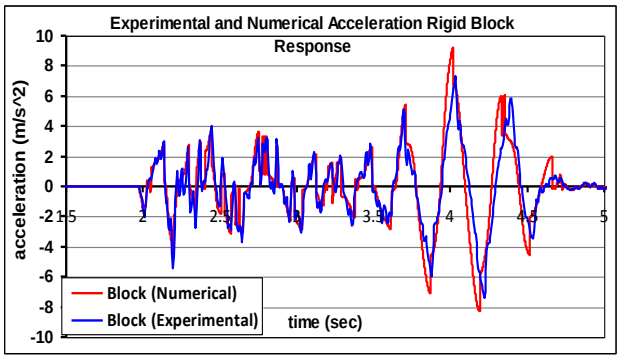

Fig. 16b. Acceleration response of moving platform and of the sliding rigid block (Test 004, 21-12-2007)

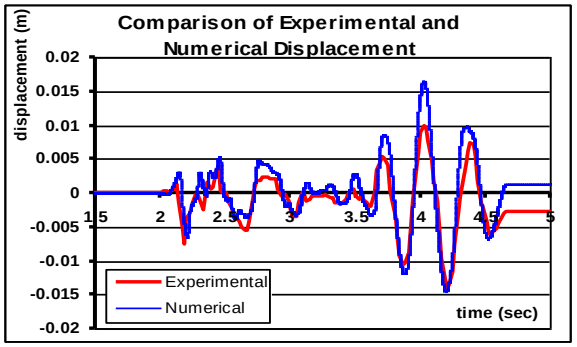

Fig. 16c. Sliding displacement response of rigid block (Test 004, 21-12-2007)

4.4 Comparison of numerical and measured response during the test employing Sinusoidal excitation 1.5Hz without spring

The comparison between predicted and measured rigid block acceleration response is presented in figures 17a,b as was done in the previous sections whereas the predicted rigid block sliding response is presented in figure 17c. The rigid block is resting this time to the moving platform without any spring link attachment, which was used in the previous sections (4.1 to 4.3). The excitation of the moving platform is initially sinusoidal 1.5Hz. As can be seen, good agreement is obtained between predicted and measured rigid block acceleration response. The predicted rigid block sliding displacement response correlates reasonably well with the one measured in the laboratory in the time domain. However, the predicted sliding displacement response, in terms of amplitude, is significantly larger than the one measured in the laboratory. It is interesting to note that the cumulative sliding displacement, which

appears as an offset from the initial zero displacement condition in the measurements, is not predicted by the software. This partly confirms the explanation given in section 3.4. that this measured cumulative (offset) sliding displacement response may be attributed to manufacturing tolerances whereby the contact surface between the rigid block and the moving platform deviates from the ideal horizontal plane.

.

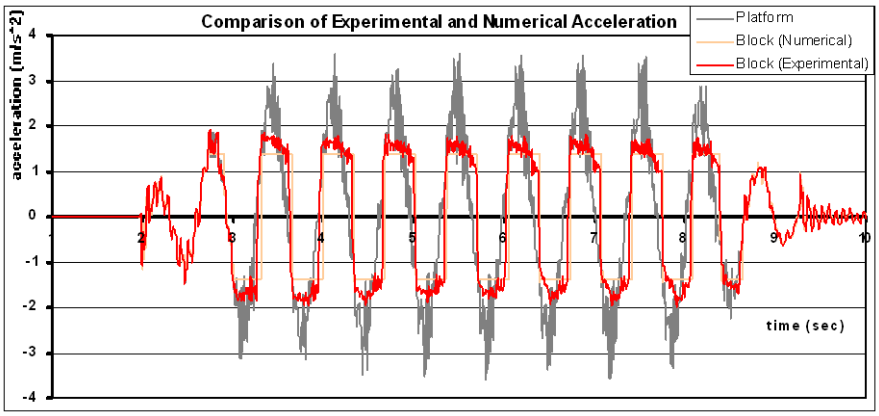

Input parameters
μst= .15
μd= .14
K (N/m)= 0
M (kg)= 248
DtF (sec)= .005
Dt (sec)= .001
TIME (sec)= 10.845

Fig. 17a. Acceleration response of moving platform and of the sliding rigid block (Test 005, 14-1-2008)

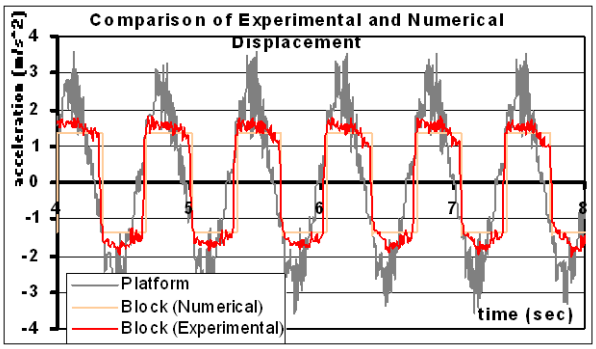

Fig. 17b. Acceleration response of moving platform and of the sliding rigid block (Test 005, 14-1-2008)

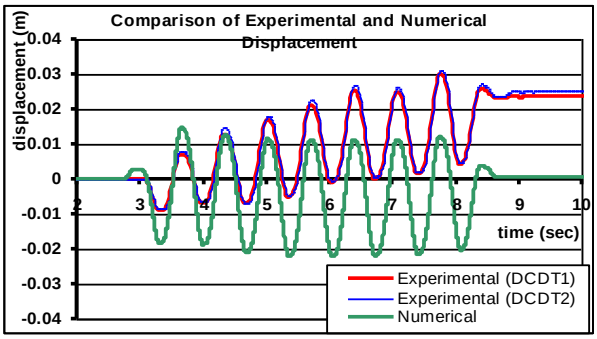

Fig. 17c. Sliding displacement response of rigid block (Test 005, 14-1-2008)

4.5 Comparison of numerical predictions with the response measured during the test employing simulated earthquake excitation without spring

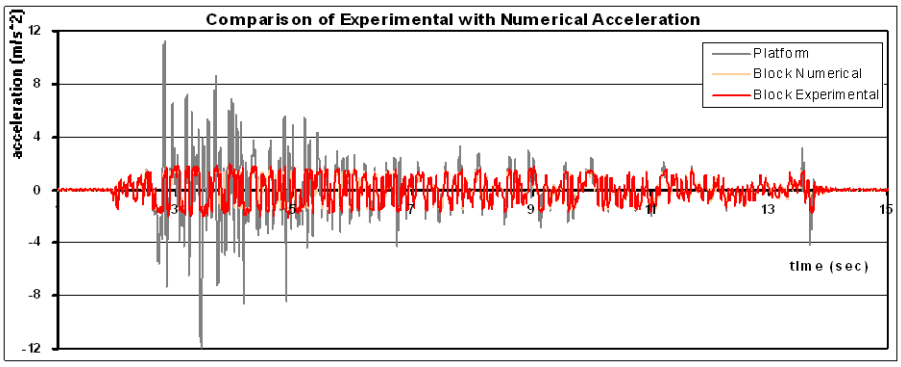

Input parameters
μst= .15
μd= .14
K (N/m)= 0
M (kg)= 248
DtF (sec)= .005
Dt (sec)= .001
TIME (sec)= 15.725

Fig. 18a. Acceleration response of moving platform and of the sliding rigid block (Test 014, 14-1-2008

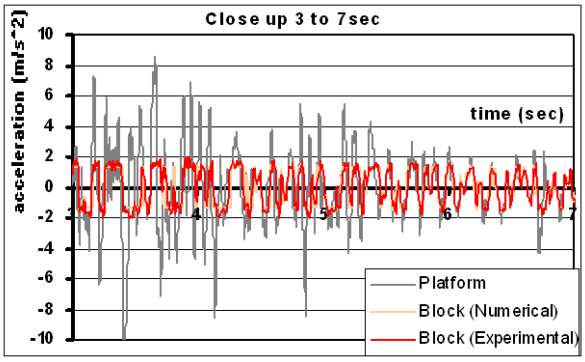

Fig. 18b. Acceleration response of moving platform and of the sliding rigid block (Test 014, 14-1-2008)

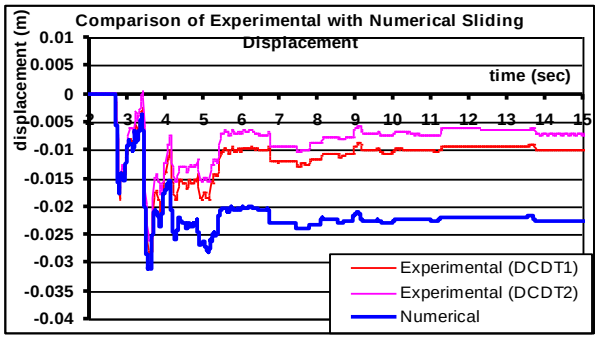

Fig. 18c. Sliding displacement response of rigid block (Test 014, 14-1-2008)

The comparison between predicted and measured rigid block acceleration response is presented in figures 18a,b as was done in the previous sections whereas the predicted rigid block sliding response is presented in figure 18c. The rigid block is resting, as in section 4.4., to the moving platform without any link employing any spring attachment; however, this time a simulated earthquake excitation is used. As can be seen, good agreement is obtained between predicted and measured rigid block acceleration response. The predicted rigid block sliding displacement response correlates reasonably well with the one measured in the laboratory in the time domain as well as in terms of maximum amplitude. It is again interesting to note that, there is a cumulative sliding displacement that appears as an offset from the initial zero displacement condition in the predicted response that is much larger than the one observed during the experiment. This observation contradicts the explanation, which was given before in section 4.4., that this measured cumulative (offset) sliding displacement response may be attributed to manufacturing tolerances whereby the contact surface between the rigid block and the moving platform deviates from the ideal horizontal plane. As an alternative explanation, these differences between predicted and measured rigid block cumulative (offset) sliding displacements may also be attributed to the integration scheme which was used by the computer software. This alternative explanation needs verification.

In figure 19, the ratio of the acceleration response spectral values based on the rigid block acceleration response over the corresponding acceleration spectral values based on the platform acceleration is plotted in the period range from 0 to 2 seconds. This is done for test 14 (14-1-2008) whereby the rigid block was subjected to a simulated earthquake motion, as is shown in figures 19a,b,c. The relevant spectral ratio values are for 5% damping and correspond to both the predicted and the observed block acceleration response.

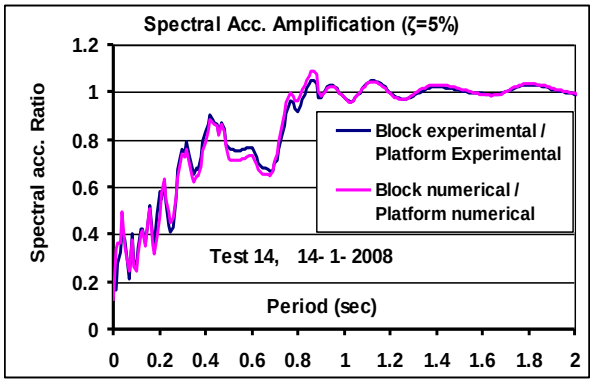

Figure 19. Ratio of response spectral values

As can be seen in this figure, these response spectral ratio values are, as expected, smaller than 1, which indicates the influence of sliding in reducing the rigid block acceleration response, as means of seismic isolation.

4.6 Comparison of numerical predictions with the response measured during a sweep test in the frequency domain.

In this section, a final comparison is performed between measured and predicted rigid block acceleration response. The developed software is utilized to perform a series of numerical solutions whereby the same rigid block with the same mass, spring stiffness and friction coefficients is used by subjecting it to a series of distinct sinusoidal excitations of the moving platform keeping the peak acceleration amplitude constant but varying the frequency of the excitation (numerical sweep test). The ratio of the maximum rigid block acceleration response over the peak acceleration of the moving platform from each numerical solution is plotted in figure 20 against the frequency of the corresponding excitation. This is done simulating three distinct physical problems representing the following:

- The tested during the experimental sequence rigid block with the certified spring (μst= 0.15 μd=0.14, M=248kg, K=100000N/m no pre-stress) , presented in sections 3.1. to 3.5.
- The tested during the experimental sequence rigid block with the certified spring (μst= 0.15 μd=0.14, K=20000N/m no pre-stress), presented in sections 3.1. to 3.5.
- The tested during the experimental sequence rigid block with the certified spring (μst= 0.15 μd=0.14, K=2000N/m no pre-stress) , presented in sections 3.1. to 3.5. This simulates a case whereby the spring link between the rigid block and the moving platform is very flexible, towards approximating a case whereby there is no spring link.

The resulting numerical values are plotted in figure 20 with solid lines whereas the corresponding experimental values are also plotted in the same figure with the dotted lines that connect the measured values (squares) at distinct frequencies during specific experiments. The following observations can be made based on the results presented in this figure.

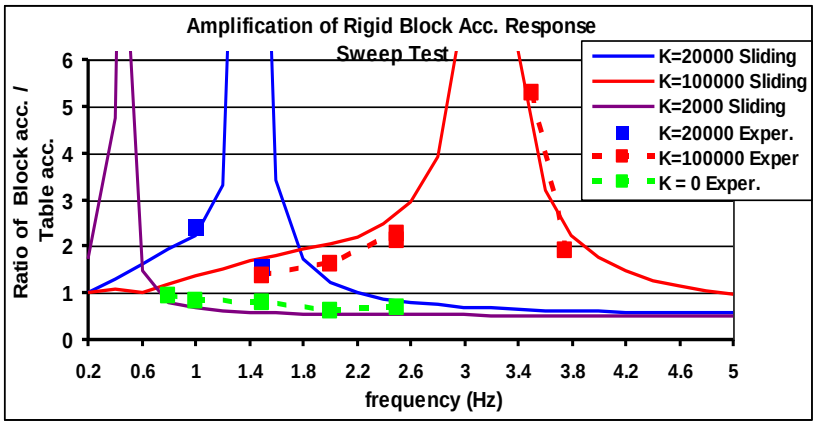

Figure 20. Comparison of measured and predicted rigid body acceleration response

a. As expected, the presence of the spring introduces an amplification in the rigid block acceleration response with amplification ratio values less than two (2), except when the frequency of the excitation is close to the resonant frequency of the spring-block dynamic system. It must be pointed out that in the examined cases apart from the friction there is absence of any other damping mechanism; moreover, the friction coefficients were measured to have relatively small values (section 2.1). The absence of any other damping mechanism apart from the friction, with small values of the coefficients of friction, can also explain the

large amplification values when the excitation frequency becomes close to the resonant frequency [1].

b. When, the value of the spring stiffness is relatively small, the amplification of the rigid body acceleration response is smaller than one (<1) in the frequency range of many practical applications in the seismic design.(for frequencies larger than 0.5Hz, or for periods smaller than 2 seconds), thus introducing in this way the well known seismic isolation of such a rigid block, which is obtained by many such sliding devices.

c. The comparison between the measured results and the predicted values in this plot exhibit relatively good agreement, especially when this comparison is done in frequencies that are not close to the resonant frequency range.

d. In the tested case whereby there is no spring between the rigid block and the moving platform the response amplification value is smaller than one (<1) in a more extended frequency range.

5 CONCLUSIONS

1. An extensive experimental sequence has been performed studying the sliding response of a rigid block linked with a spring, having a wide variety of stiffness values, to a moving platform and being subjected to sinusoidal and simulated earthquake excitations. There was no other damping mechanism apart from the friction between sliding block and moving platform with relatively low values of the coefficient of friction. The experimental results have shown that when sliding of this rigid block is permitted then its peak acceleration response is moderately amplified, provided that the excitation frequency is not close to the resonant frequency range of the block-spring dynamic system. This is particularly true for earthquake excitations and for relatively flexible spring-links thus achieving in this way a type of seismic isolation for the rigid block.

2. This sliding response of the rigid block is accompanied by sliding displacements that can be of relatively large amplitude, when the stiffness of the spring that links the rigid block with the moving platform is relatively low. This sliding displacement response is accompanied by a cumulative sliding displacement, which may result in a permanent sliding displacement of considerable amplitude at the end of the excitation. The amplitude of the sliding displacement response decreases with the increase of the spring stiffness, when the excitation is not close to the resonant frequency of the spring-block dynamic system.

3. A computer software was developed in order to predict this rigid block sliding response. The numerical predictions were validated by comparing them to a large number of experimental measurements. As can be seen from this comparison, the numerical predictions confirm all the behavioral observations of the studied phenomenon, as they were recorded during this extensive experimental sequence.

4. The numerically predicted rigid block acceleration response is in good agreement with the measured values for all examined cases of spring stiffness and for both the sinusoidal as well as the simulated earthquake excitation of the moving platform.

5. The numerically predicted rigid block sliding displacement response exhibited in some cases good agreement with the measured values. However, in some other cases the deviation between predicted and measured rigid body sliding displacement response values were significant (of the order of 100%). It is interesting to note the cumulative sliding displacements that appear as an offset from the initial zero displacement condition; this is successfully reproduced by the predicted response only in some cases. Possible explanations that are given for this are manufacturing tolerances, whereby the contact surface between the rigid block and

the moving platform deviates from the ideal horizontal plane, as well as the integration scheme that is included in the computer software.

6. Despite the limitations of the predicted results it is believed that the developed software, although it deals with a complex problem in a relatively simple way, it can be useful in the preliminary design stages of structural systems with the sliding capability at their support.

REFERENCES

[1] Anil K. Chopra, "Dynamics of Structures: Theory and Applications to Earthquake Engineering", 2006

[2] M. Aslam et al. (1975), Sliding response of rigid bodies to earthquake motions, Rep. No. LBL-368, Lawrence Berkeley Laboratory, University of California.

[3] B. Westermo and F. Udwadia, (1983), Periodic response of sliding oscillator system to harmonic excitation, Earth. Engin. and Str. Dyn., 11, pp.135-146.

[4] C.J. Younis and I.G. Tadjbakhsh, (1984), Response of sliding rigid structure to base excitation, J. of eng. Mech., ASCE 110, pp. 417-432.

[5] H. W. Shenton and N. P. Jones (1991), Base excitation of rigid bodies, I: Formulation, J. of Eng. Mechanics, ASCE, 117(10), pp. 2286-2306.

[6] M. Demosthenous, (1994), Experimental and numerical study of the dynamic response of solid or sliced rigid bodies, Ph. D. Thesis, Dept. of Civil Engineering, Aristotle University of Thessaloniki, Greece.

[7] G.C. Manos and M. Demosthenous, (1990), The behavior of solid or sliced rigid bodies when subjected to horizontal base motions, Proc. of 4th U.S. National Confer. on Earthquake Engineering, Vol. 3, pp41-50.

[8] G.C. Manos and M. Demosthenous, (1993), Dynamic Response of Sliced Rigid Bodies Subjected to Harmonic Base Excitations, SMIRT-12, Vol. K1, K11/3, pp. 313-318.

[9] G. C. Manos et al. (2000), Study of the dynamic and earthquake behavior of models of ancient columns and colonnades with and without the inclusion of wires with energy dissipation characteristics", presented at the 12th WCEE, Auckland, New Zealand.